

Dynamical incompatibilities in paced finger tapping experiments

Ariel D. Silva,^{1, 2} Claudia R. González,¹ and Rodrigo Laje^{1, 2, 3, *}

¹Universidad Nacional de Quilmes, Departamento de Ciencia y Tecnología, Sensorimotor Dynamics Lab, Argentina
²CONICET, Argentina

³Universidad de Buenos Aires, Facultad de Ciencias Exactas y Naturales, Departamento de Computación, Argentina
(Dated: December 30, 2025)

The behavioral description of the sensorimotor synchronization phenomenon in humans is exhaustive, mostly by using variations of the traditional paced finger-tapping task where a participant is instructed to tap along with a periodic sequence of brief tones. This task helps unveil the inner workings of the error-correction mechanism responsible for the resynchronization after a perturbation to the period of the stimuli sequence. Yet, fundamental contradictions still exist among different works in the literature. One of such contradictions only emerges after comparing the two most-common period perturbation types: step changes and phase shifts. The stimulus sequence is exactly the same in both perturbation types up to and including the (unexpected) perturbed stimulus. Why then would the timing of the next response be different between perturbation types, as observed? The explanation lies in the buildup of different temporal contexts during the experiments that recalibrate the error-correction mechanism. Here we show, both experimentally and theoretically, that responses to different perturbation types are dynamically incompatible when they occur in separate experiments. That is, they can't be represented by the same underlying dynamical system, thus explaining many contradictory results and the difficulty in reproducing both types of perturbations with a single mathematical model. On the other hand, if both perturbation types are presented at random during the same experiment then the responses are compatible with each other and can be construed as produced by a unique underlying mechanism. We conclude that a single underlying dynamical system can represent the response to all perturbation types, signs, and sizes, which is nevertheless recalibrated by temporal context. Our results offer a ground for performing better comparisons in paced finger tapping and extend the usable range of data beyond the perturbed stimulus and into the information-rich resynchronization phase.

Keywords: Sensorimotor synchronization; Period perturbations; Dynamical systems; Time-delay embeddings

I. INTRODUCTION

In the study of time processing and temporal cognition on the scale of hundreds of milliseconds, the last two decades have brought significant advances in describing behavior and understanding their neural bases and developmental stages [1–5]. Recognizing that time is processed on multiple time scales is key to understanding how the brain and body coordinate during movement planning and control [6]. Within this time scale lies sensorimotor synchronization (SMS), that is, the ability to adjust our movements to match a periodic external stimulus that is the basis of human activities such as music and dance [7–11]. Research on SMS as a potential diagnostic marker in neurodegenerative diseases has seen a rise in the last decade [12, 13] for diseases where motor dysfunction is a primary symptom like Parkinson's [14, 15] and even others where motor deficits occur later, like Alzheimer's [16, 17] and mild cognitive impairment [18, 19].

The most basic paradigm for investigating SMS is paced finger tapping, in which subjects are asked to synchronize to an external metronome (usually a periodic sequence of brief tones). Within this framework, researchers often introduce unexpected changes to the

interstimulus interval (ISI) to study how the system responds. This task has enabled key advances, such as the identification of perceptual and motor components involved in the resynchronization process following a perturbation [20], as well as the observation of an asymmetry in the way lead and lag synchronization errors are processed, consistent with a previously documented behavioral asymmetry [21].

Despite this progress, key questions remain unresolved. It is generally accepted that average synchronization and its recovery after a perturbation are sustained by an error correction mechanism [7, 9, 11, 21, 22]. Although linear models have long been used to describe this resynchronization process [8], more recent analyses of time series under different perturbation types and sizes suggest that this mechanism exhibits nonlinear characteristics [10, 21, 22]. Other experimental results also support the need to abandon linear models in favor of more complex descriptions [23–31]. This change of perspective could have relevant implications for experimental design, the methodologies used for data analysis, and the development of diagnostic tools [10, 11, 22].

In this work, we reanalyzed SMS data and showed that responses to different perturbations are experimentally incompatible with each other in terms of a putative underlying dynamical system, unless they are presented in the same experiment. We also used a previously developed nonlinear model [10] to fit the data and theoretically

* Corresponding author: rlaje@unq.edu.ar

demonstrated this incompatibility. Our results allow us to reconcile contradictory experimental data and reinterpret the historical difficulty that mathematical models of SMS have had in reproducing, with a single set of parameters, the response to perturbations from different experiments.

II. RESULTS

A. Experimental time series from pure contexts are incompatible with each other

In a previous study, we performed an experiment to investigate how the perturbation context influences resynchronization dynamics during a finger-tapping task [11]. The task consisted of subjects tapping their fingers to the beat of a periodic sequence of auditory stimuli. During this task, period perturbations were introduced to analyze the adaptive response of the underlying error-correction mechanism to unexpected changes in the temporal pattern.

One of the main motivations of the cited study was to evaluate whether the context in which the perturbations occur modifies the resynchronization behavior. To this end, two types of perturbations widely used in the literature on paced finger tapping were employed: step change (SC) perturbations and phase shift (PS) perturbations. In SC perturbations the period changes abruptly once at an unexpected moment in the sequence. In PS perturbations the period changes twice, returning to its original value in the following step [9].

A context factor was defined based on the way the perturbations were presented: “pure” context (only one type of perturbation) and “combined” context (random alternation of the two perturbation types on a trial-by-trial basis). It was observed that the way participants adjust their responses depends on the context. In a pure context, the system adapts specifically to the pattern of each type of perturbation. In a combined context, however, it adopts an intermediate strategy that allows it to respond to both types of perturbations. Our question is whether the responses to SC and PS perturbations in pure contexts are compatible with each other; that is, whether they can be produced by the same dynamical system.

Figure 1 shows how participants resynchronize after SC and PS perturbations in pure (panel a) vs combined (panel c) contexts. We plot the asynchrony e_n , that is the time difference between corresponding response R_n and stimulus S_n occurrences ($e_n = R_n - S_n$). The unexpected perturbations occur at $n = 0$ where the asynchrony takes a large value (a forced error); participants return to baseline after resynchronization.

To determine the degree of compatibility between responses to different types of perturbations, we calculated the experimental phase space for each time series using a variant of the time-delay embedding [32] (see Appendix). The results are shown in Figure 1 (panels b,d). In a pre-

vious work [10] we demonstrated that, although asynchrony e_n can be precisely defined and measured in operational terms and it is the most fundamental observable in an isochronous paced finger-tapping experiment [33], it is not suitable as a modeling variable in situations involving period perturbations. That’s why we plot the embeddings in terms of the related variable “predicted asynchrony” p_n (see Appendix). This variable is well-defined in the presence of period perturbations and allows us to interpret the geometrical organization of the phase space with the tools of Dynamical Systems theory.

In the pure context (top right panel), the flow in the upper left quadrant associated with SC and PS perturbations intersect each other. This is clear evidence of incompatibility between them, since the flow departing from the intersection points in different directions. In a deterministic 2D dynamical system with no hidden variables, a single point in phase space can’t have two different futures [9]. This holds true for both small and large perturbations. We emphasize that this result is independent of any particular mathematical model.

On the other hand, in the combined context (bottom right panel), the flows exhibit a smooth organization, with trajectories that do not drastically intersect as before. It is worth noting that the data for the 20 ms perturbation exhibit high variability [11], which could explain a slight overlap at noise level for this perturbation size. Considering this, it can be concluded that data in the combined context suggest a common dynamics (for both small and large perturbations). This shows the plausibility of a shared underlying solution in the combined context capable of simultaneously describing the responses to all perturbation types, signs, and sizes.

In summary, these results show that responses after SC and PS perturbations in pure conditions are incompatible with each other. While in the combined context the flow accommodates smoothly, the pure contexts reveal specialized responses that cannot be reconciled under a single model without separate fittings. This observation has methodological implications for future studies of sensorimotor synchronization and provides empirical evidence for an underlying mechanism that can represent diverse types, sizes, and signs of perturbation with a single set of terms and parameters, but which is calibrated by the statistical history of the environment.

B. Mathematical models fitted to pure conditions are incompatible with each other

To show how the experimental incompatibility described in the previous section manifests itself in a mathematical model, we consider the following nonlinear dynamical system:

$$\begin{aligned} p_{n+1} &= ae_n + b(x_n - T_n) + \beta e_n(x_n - T_n)^2 \\ x_{n+1} &= ce_n + d(x_n - T_n) + \delta e_n^2 + T_n \end{aligned}$$

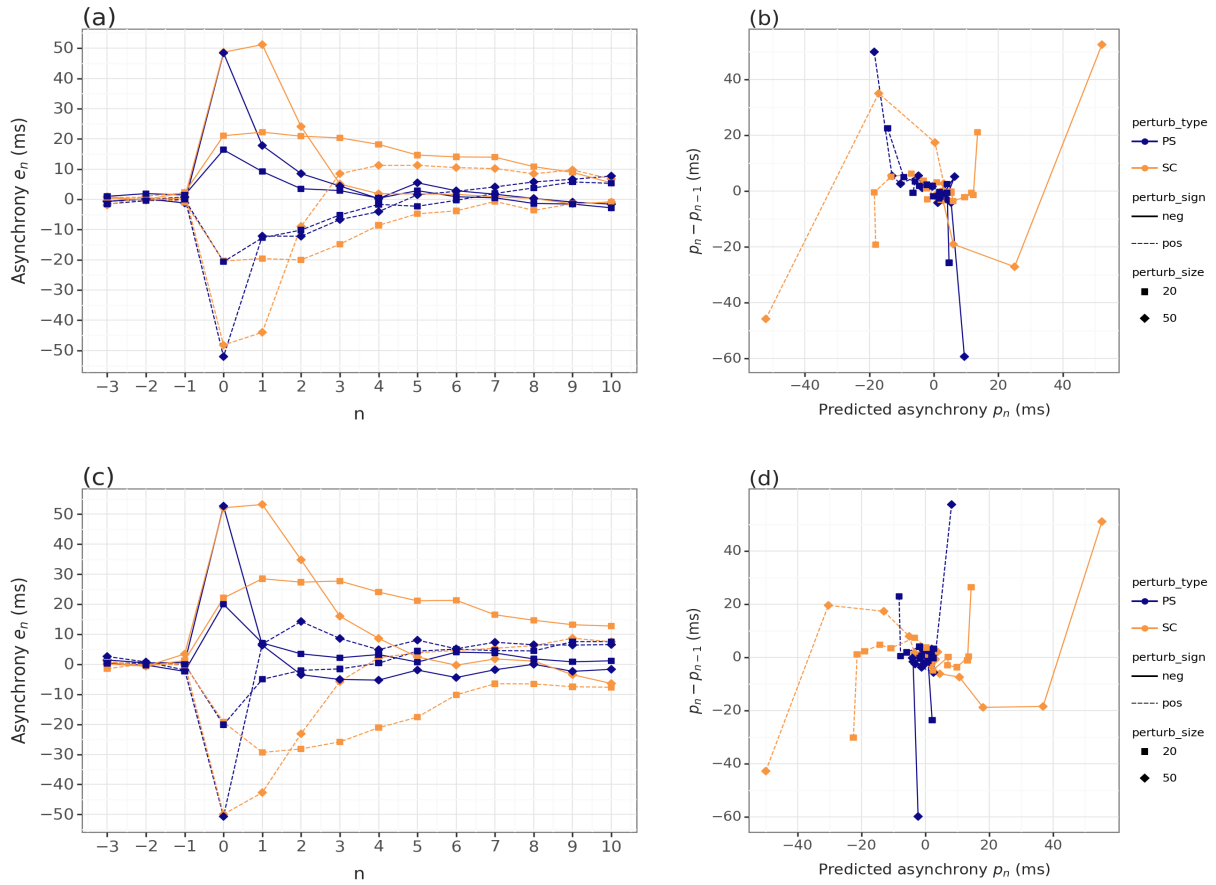


FIG. 1. Crossings in the reconstructed phase space point to an incompatibility between SC and PS from pure contexts. Left: experimental time series. The (unexpected) perturbations occur at $n = 0$; the forced error is reflected in a large asynchrony value, on average opposite to the perturbation size ΔT . Participants gradually recover synchronization afterwards. Right: Time-delay embeddings (SC: $1 \leq n \leq 8$; PS: $2 \leq n \leq 8$). Top: Pure context. A clear crossing of trajectories between SC (orange) and PS (blue) occurs in the top left quadrant of the embedding. Bottom: Combined context. Mean across participants; error bars not shown for clarity.

(see details in the Appendix). This is a simplified version of a previous model [10].

To test the incompatibility hypothesis between perturbation types in pure contexts, two independent fittings were performed, grouping the experimental data according to perturbation type (SC pure vs PS pure; we used the Differential Evolution (DE) global optimization function from the SciPy library, implemented using a script in Python; see Appendix).

If the incompatibility hypothesis were true, we should find that the fittings yield incompatible phase spaces, whereas if it were false, the fitted models should have flows with compatible dynamics.

Results are plotted in Figure 2. The left panels show the experimental time series in black and the corresponding fitted model time series in blue (PS in pure context) and orange (SC in pure context). Selected trajectories from the models' phase spaces are plotted on the right panel. It is clear that the trajectories of SC and PS perturbations cross each other, pointing to incompatible

underlying systems.

C. Parameter distributions of different perturbations in pure context do not overlap

To statistically evaluate the incompatibility hypothesis, we applied the fitting algorithm 200 times to each pure condition independently (SC in pure context and PS in pure context). Our goal was to compare the resulting parameter distributions and determine whether the overlap between them is negligible (further supporting the idea of incompatibility, there are no shared parameter values) or, on the contrary, they clearly overlap (i.e. they are compatible, since they share possible parameter values).

The resulting distributions are shown in Figure 3. It is evident that, for parameter a , there is a partial overlap between SC in pure context and PS in pure context, which might suggest the plausibility of a common so-

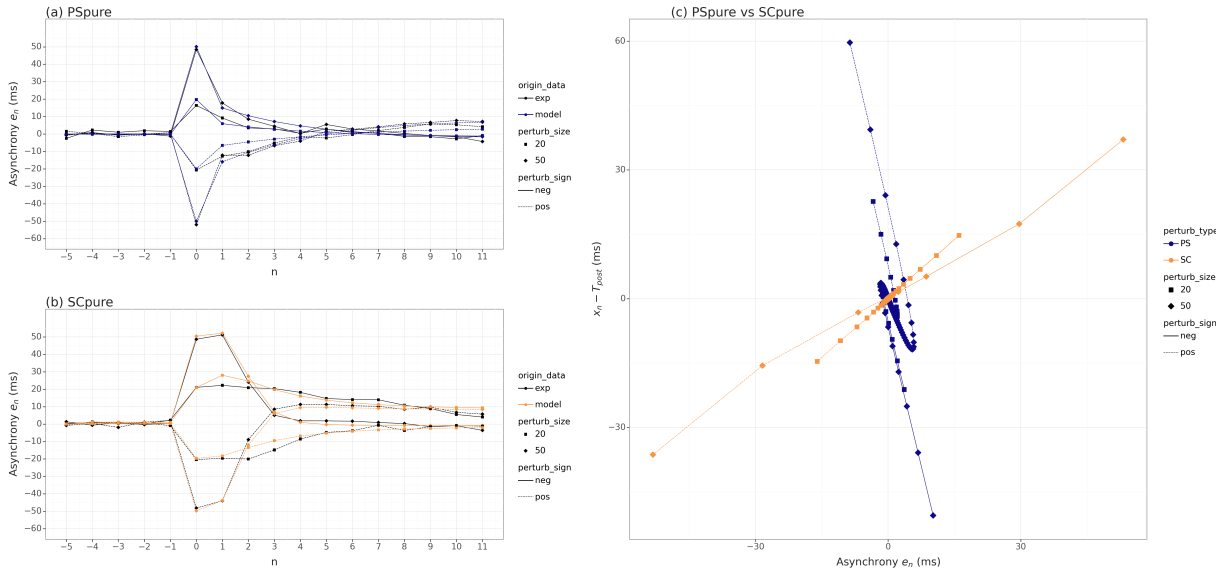


FIG. 2. Model fitting to the incompatible experimental time series leads to model phase spaces that are also incompatible to each other. (a) and (b): Separate model fittings (color) to SC and PS from pure contexts (black). (c) Phase space of the fitted models. Incompatibility is manifested as clear crossings between trajectories of different colors.

lution. However, the overlap vanishes in the remaining parameters. Particularly for parameter β , the overlap is negligible between the corresponding populations, ruling out the possibility of finding a single set of parameters that could reproduce both types of perturbation. See the distributions of all parameters in Figure 6.

This result theoretically supports the hypothesis of incompatibility between SC and PS in pure contexts, previously proposed based on the experimental incompatibility observed in Figure 1. Consequently, it is concluded that, in the pure context, the model requires separate fits for each type of perturbation.

To quantify the extent of overlap between the obtained distributions, we defined the statistic O_{obs} (see Appendix) that measures how much two distributions empirically overlap based on the range of values they both share and, therefore, that would allow a joint fit of the model.

The distributions of parameter a in Figure 3a have a large overlap: $O_{obs} = 71.5\%$. On the other hand, the distributions of parameter β in Figure 3b display a very small overlap: $O_{obs} = 3.7\%$. This allows us to conclude that a narrow model tuning should be necessary to reproduce both SC in pure context and PS in pure context with a single set of parameter values, contrary to the common observation of this very robust synchronization behavior.

D. Parameter distributions from different perturbations in a combined context do overlap

The counterpart to the incompatibility hypothesis between SC perturbations and PS perturbations in pure

contexts is that when these perturbations occur in a combined context instead, they are indeed compatible, as shown experimentally in Figure 1 (c,d). To further support the incompatibility hypothesis, then, we should show that a similar analysis but with combined context data results in the fitted parameter distributions showing overlap between PS and SC for all model parameters.

Figure 4 shows the results. We performed separate model fittings to SC and PS from combined contexts this time and their distributions overlap for all parameters. This result reinforces the hypothesis of solution compatibility between SC and PS in combined context, previously proposed based on the flow compatibility observed in Figure 1. This means that we can find a single set of model parameter values that reproduce both types of perturbation at once, with no fine tuning needed.

As in the previous section, the extent of overlap was quantified using O_{obs} . All parameter distributions show a large overlap between SC and PS, with a the minimum overlap of 64% (panel d) and a maximum overlap of 73% (panel a).

E. Joint fitting: pure context fares worse than combined context

An additional piece of converging evidence regarding the incompatibility between SC and PS in pure contexts comes from the joint (rather than separate) fitting of experimental conditions. By joint fitting we mean fitting a single set of parameters to both perturbation types at once. If SC in pure context and PS in pure context are shown to be incompatible when separate fittings are performed (section II C) while in the combined context they

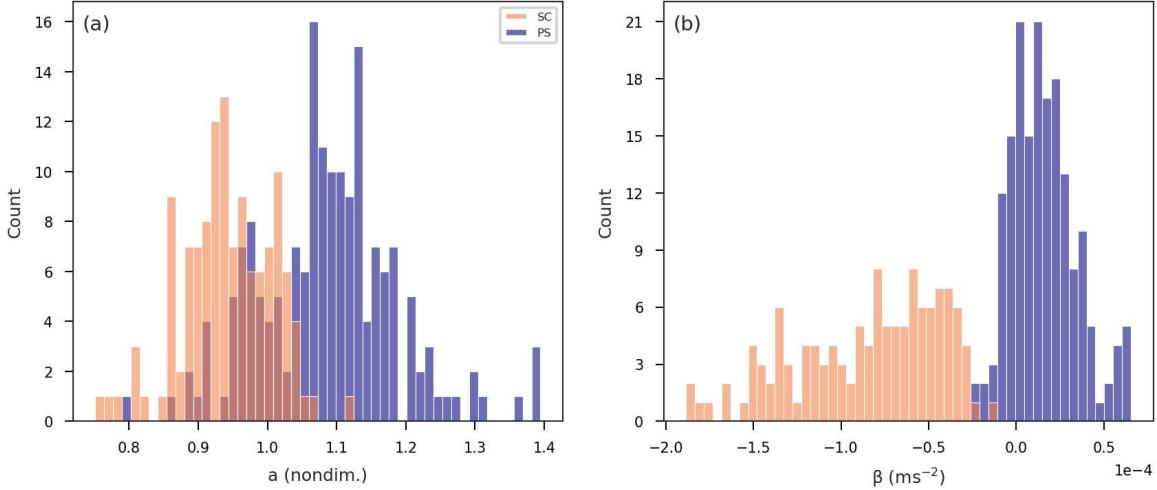


FIG. 3. Separate model fittings to SC in pure context and PS in pure context don't share common parameter values for all parameters. (a) There is some overlap between the obtained distributions of parameter a . (b) Distributions of parameter β , however, show negligible overlap.

are compatible (section II D), then an even stronger case would be built by showing that joint fitting of SC and PS from pure contexts is much worse than joint fitting of SC and PS from combined context.

We performed 200 independent joint fittings for each condition (that is, 200 joint fittings of SC and PS in pure context, and 200 joint fittings of SC and PS in combined context) and compared the quality of the fitting by looking at the resulting values of the fitting loss function (the objective function to be minimized, chosen to be the Euclidean distance between times series; we call it "distance"; see Appendix). Figure 5 shows that the distances obtained in the combined context are systematically smaller than those in the pure context, with two distinct distributions. All distance values in the pure context were greater than 51 ms with a median of 63 ms, while all distance values in the combined context were less than 49 ms with a median of 46 ms. To assess statistical significance, we ran a non-parametric Mann-Whitney-Wilcoxon test resulting in significant differences between pure and combined context distributions with a very large effect size ($U = 39402, p = 10^{-10}$, Cliff's delta = 1, mean of Cliff's delta by bootstrap = 1 with 95% CI = [1, 1]).

Since a smaller distance indicates a better model fit (i.e., a smaller value of the fitting loss function), these results confirm that the joint fitting of both types of perturbation in the combined context is closer to the experimental time series than in the pure context. In other words, we interpret this result as the time series in the pure context being more difficult to fit at once because they stem from incompatible systems.

F. Parameter correlations and model overparameterization

The pairwise joint distributions of fitted parameter values (Figures S1 and S2 in Supplemental Material [34]) show that there are some correlations between them, especially among the linear parameters, suggesting that the model is overparameterized. This behavior suggests that the results could be adequately explained by an even simpler version of the model where some of the linear parameters are expressed as a function of others, thus reducing the degrees of freedom. A slight correlation between linear and nonlinear parameters was also observed in some cases.

For the joint fitting of PS and SC in pure context in particular, no correlation between parameters was observed. The absence of correlations implies that the model needs to use all parameters independently to reproduce the data, in contrast to the individual fittings within the same context (SC in pure context and PS in pure context). That is, the model capabilities are strained to their limits and, even in that case, the fitting has a low quality (large fitting loss function values).

On the other hand, the nonlinear parameters (β and δ) do not show clear correlations with each other, which indicates that the nonlinear part is appropriately parameterized.

A criticism could be raised that, if the model is overparameterized, then any correlation between parameters would prevent us from concluding about incompatibility. This is not true, as we show in section A 8 in the Appendix.

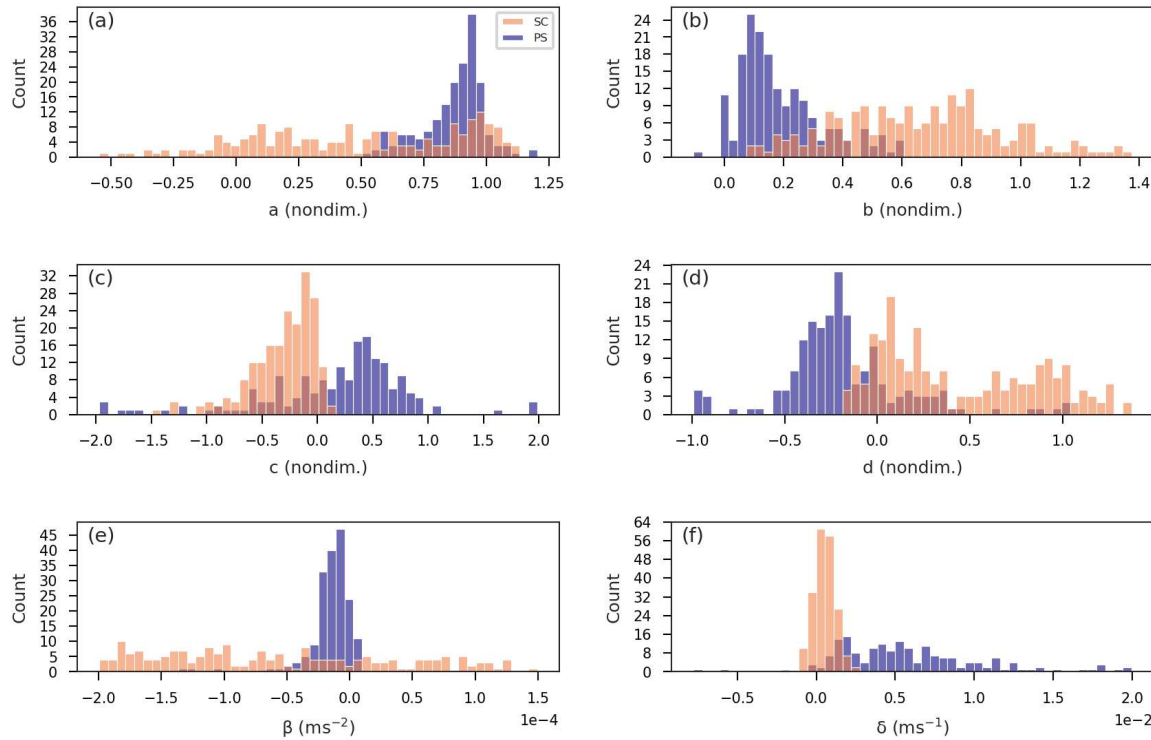


FIG. 4. Parameter value distributions from SC and PS in combined context. Separate fittings for SC and PS lead to overlapping distributions for all six model parameters.

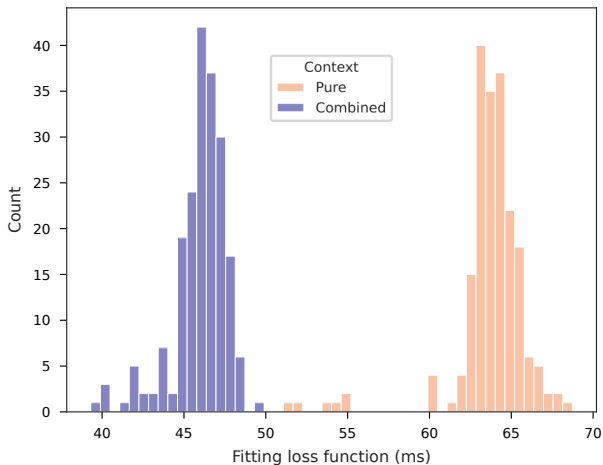


FIG. 5. Joint fitting of SC and PS perturbations from pure context show lower-quality fits (i.e., larger values of the fitting loss function) than its counterpart from combined context.

III. DISCUSSION AND CONCLUSION

Basic findings

In this work we showed that responses to period perturbations of different types in paced finger tapping (step changes vs phase shifts) are dynamically incompatible when they occur in different experiments, due to the existence of a previously shown context effect [11]. This led us to conclude, both empirically and theoretically, that they can't be produced by a single underlying error-correction mechanism. When they occur in the same experiment, however, they are compatible with each other and a single mathematical model can be successfully fitted to the whole dataset. We interpret these results as mounting evidence about the plausibility of a unique underlying nonlinear mechanism supporting the resynchronization behavior for all perturbation sizes, signs, and types, which nonetheless is tuned to the specific temporal context of an experiment. A summary of the converging evidence supporting our claims can be found in Table I.

We reached our conclusions by specifically analyzing the resynchronization phase, that is the transient part of the response between the preperturbation and postperturbation baselines. As we previously showed [9–11, 22], many defining aspects of behavior are only evident in this

information-rich transient. Building on this research programme, the present study further establishes the correct way of comparing the transients when they come from different perturbation types—we need to control for the perturbation context.

Quantitative tools supporting clinical assessment of motor timing deficits

Clinical assessment of fine motor function typically involves measures of motor control that, although based on standardized rating scales, are subjective [12]. On the other hand, although some neuropsychological assessment tools are quantitative, they measure only very basic quantifiable aspects of timing behavior. For example, the Finger Tapping Test (FTT, also known as Finger Oscillation Test) in the Halstead-Reitan neuropsychological test battery [35] measures the number of taps a patient performs in a fixed 10-second interval. Traditional measures from the finger tapping literature like average asynchrony and standard deviation, and intertap intervals [8] are absent, and research on their diagnostic capabilities is scarce [12]. Models are even less used [27]. More work is needed to understand the underlying mechanism so we can define appropriate quantitative measures of behavior to distinguish health from disease.

Conflicting experimental data explained

Our results offer a unified view of conflicting experimental data in the finger tapping literature: the timing of the first response after a perturbation is different depending on the perturbation type, despite that the stimulus sequence up to and including the perturbation is the same. This fact has been interpreted as due to the participant’s “intentions and expectations” [36] after noting different phase correction responses (PCR) to phase shift perturbations and event-onset shift perturbations. We emphasize that our results show that these different “expectations” are not mere changes to some correction coefficient but are represented and produced by incompatible dynamical systems. For more examples of conflicting experimental data, see our literature review on SC and PS perturbations in Ref. [11]. At the same time, our account offers an explanation for the absence of model fittings in the finger tapping literature representing different perturbation types with a single set of parameter values—if the data are incompatible, then no single model can satisfactorily fit them all. The usual way is to fit a model separately for every experimental condition, as we described in Ref. [10]. Even our own previous work [9] showed some modelling difficulties: in order to get high quality model reproduction and predictions across all perturbation types, signs, and sizes with a single model, the first response after perturbation needed to be removed from the fitting.

A single, nonlinear underlying mechanism

Our results challenge the proposed idea of “different mechanisms for different perturbation types” [7, 8]: that is, the proposed existence of two different mechanisms, named phase correction and period correction, that are selectively engaged depending on the perturbation type. According to this proposal, the phase correction mechanism only is active in phase-shift perturbations, while both the phase correction and period correction mechanisms are active in step-change perturbations [7, 8, 37]. These mechanisms, in addition, are associated with separate model equations. Our results from the combined context, showing that the SC and PS experimental data are compatible with each other and are both well fitted by a single model with both model equations at play, warrant a revision of this idea. When participants are exposed to both perturbation types at random in the same experiment, they don’t seem to select different strategies but a single, intermediate strategy [11] represented by a unique set of model parameter values.

Neural correlates and mathematical representation of sensory expectation

In a version of the reaching task, it was very recently demonstrated [38] that when humans and monkeys are probabilistically cued about the direction of an upcoming mechanical perturbation, they incorporate this information to correct and improve their responses. Importantly, when this information was accumulated over trials, brain areas related to motor preparation and execution showed neural correlates of this information, suggesting that at least the motor aspects of the underlying mechanism change their neural representation depending on context. The accumulation of sensory expectation occurs very similarly in our experimental data, where the perturbation type was implicitly cued as the participants were not told what perturbation type they would be presented with (participants in “pure” context: either SC or PS alone; participants in “combined” context: SC and PS in randomly interspersed trials). Although research on the neural correlates of SMS has seen a surge in recent years (see Discussion in Ref. [11], there are still many unexplained fundamental aspects to it and neural-based mathematical models are lagging behind. Our work shows that sensory expectations can be explicitly and quantitatively described by a single set of parameter values of a behavioral mathematical model that reproduces all data in an experiment.

ACKNOWLEDGMENTS

This work was supported by Universidad Nacional de Quilmes (Argentina, grant PUNQ #53/1028) and CONICET (Argentina).

	Embedding and phase space	Parameter distributions	
		Separate fitting	Joint fitting
Pure context	SC and PS incompatible (trajectories cross; Figs. 1b and 2c)	SC and PS incompatible (non-overlapping distributions; Fig. 3)	SC and PS incompatible (low-quality fitting results; Fig. 5)
Combined context	SC and PS compatible (smooth trajectories; Fig. 1d)	SC and PS compatible (overlapping distributions; Fig. 4)	SC and PS compatible (high-quality fitting results; Fig. 5)

TABLE I. Summary of converging evidence supporting the incompatibility hypothesis between SC and PS perturbations in pure contexts, and compatibility in combined context.

CRediT AUTHOR CONTRIBUTIONS

A.D.S.: Data curation; Formal analysis; Investigation; Software; Visualization; Writing—original draft; Writing—review & editing. C.R.G.: Formal analysis; Investigation; Writing—review & editing. R.L.: Conceptualization; Formal analysis; Funding acquisition; Methodology; Supervision; Visualization; Writing—review & editing.

DATA AND CODE AVAILABILITY

Data and code to reproduce all our analyses and figures are available in the Sensorimotor Dynamics Lab’s website <http://www.ldsmlab.unq.edu.ar/Incompatibilities2026> and Github repository: <https://github.com/SMDynamicsLab/Incompatibilities2026>

Appendix A: Methods

1. Experimental data and task description

The experimental data analyzed in this study was previously published [11]. The objective was to determine whether the perturbation context influences the resynchronization phase following a tempo perturbation in a finger-tapping task with a metronome. Participants ($N = 71$; 33 women; all right-handed; ages 18–63) were instructed to tap with their fingers to an auditory rhythm and maintain average synchrony. Upon the appearance of a perturbation, they were instructed to regain synchrony without interrupting the tapping. A trial consists of a sequence of 35 brief tones with a baseline interstimulus interval $T = 500$ ms and their responses. A period perturbation (i.e., an unexpected change to the baseline interstimulus interval) could occur at a randomly chosen step n in the range 17–22. Steps were renumbered afterwards such that the perturbation occurs at $n = 0$.

Two perturbation types were used: Step changes (SC), where the stimulus period is abruptly modified by an amount ΔT at a random step of the sequence; and phase shifts (PS), where the period changes at two consecutive steps, first by $+\Delta T$ and then by $-\Delta T$, thus returning to its original value. Perturbations could be positive ($\Delta T >$

0, “pos”) or negative ($\Delta T < 0$, “neg”), with a magnitude of either 20 or 50 milliseconds.

In addition, the subjects were grouped into two contexts. In the “pure” context participants were exposed to only one type of perturbation (Group 1, SC perturbation; Group 2, PS perturbation; both groups with 20 and 50 ms perturbation magnitudes). In the “combined” context participants were exposed to both types of perturbation, randomly interspersed (Group 3, 50 ms magnitude; Group 4, 20 ms magnitude).

The experimental design was fully factorial, with factors Context (pure and combined) \times Type (SC and PS) \times Sign (pos and neg), with additional isochronous control conditions ($\Delta T = 0$).

2. Reconstruction of the experimental phase space via embeddings

The basic experimental data is the observed asynchrony e_n , that is the time difference between corresponding occurrences of responses R_n and stimuli S_n :

$$e_n = R_n - S_n \quad (A1)$$

where n is the response/stimulus number along the sequence. The variable e_n , however, is ill-defined when the interstimulus interval changes. Based on our previous work [10], we switch to a variable that is more appropriate in the presence of period perturbations: the predicted asynchrony p_n , defined as

$$p_n = e_n + \Delta T \quad (A2)$$

where ΔT is the size of the period perturbation. This simple relationship between e_n and p_n is best conceptualized by realizing that, when an unexpected period perturbation ΔT occurs at step n in the sequence, the asynchrony value predicted by the participant p_n will not be the same as the actually observed value e_n due to the experimental manipulation [10].

Previous work showed that the error-correction mechanism underlying resynchronization after a period perturbation is best described by a dynamical model with two variables [9, 10]. The embedding technique [22, 32] allows

us to reconstruct a 2D phase space from the experimental time series of the asynchrony e_n , after switching to the more appropriate variable p_n as described above. We defined the following time-delay embedding: predicted asynchrony (p_n) on the horizontal axis vs difference between consecutive predicted asynchronies ($p_n - p_{n-1}$) on the vertical axis, averaged across subjects. The post-perturbation baseline was subtracted from all values to show convergence to the new equilibrium.

In order to prevent visual cluttering, we avoid plotting pre-perturbation and post-perturbation baseline data and instead plot data from the resynchronization phase only (SC: $n = 1$ through 8; PS: $n = 2$ through 8). In this way we also avoid showing data from different period values in the same plot.

3. Mathematical model

We model the experimental data with a single nonlinear dynamical system proposed in a previous work [10]. In this work we simplified it to include two nonlinear terms only:

$$\begin{aligned} p_{n+1} &= ae_n + b(x_n - T_n) + \beta e_n(x_n - T_n)^2 \\ x_{n+1} &= ce_n + d(x_n - T_n) + \delta e_n^2 + T_n \end{aligned} \quad (\text{A3})$$

where e_n is the actually observed asynchrony at step n (Eq. A1); p_n is the predicted asynchrony (Eq. A2); and x_n is a variable of dynamical origin needed to reproduce the behavior [9, 10]. The metronome is represented by the interstimulus interval T_n whose value can be set by the experimenter. An SC perturbation occurring at $n = 0$ changes the metronome period once at $n = 0$ ($T_n = T_{base}$ for $n < 0$ and $T_n = T_{base} + \Delta T$ for $n \geq 0$); a PS perturbation changes it twice ($T_n = T_{base}$ for $n < 0$, $T_n = T_{base} + \Delta T$ at $n = 0$, and back to $T_n = T_{base}$ for $n \geq 1$) [9].

4. Model fitting

The model was fitted to the data using the Differential Evolution function from the SciPy library in Python. We defined the fitting loss function as the Euclidean distance between the experimental time series and the corresponding model time series:

$$dist = \sqrt{\sum_{n=-5}^{11} (e_n^{(exp)} - e_n^{(model)})^2} \quad (\text{A4})$$

where $e_n^{(exp)}$ represents the experimental values of the asynchrony and $e_n^{(model)}$ the values predicted by the model at every step n in the sequence.

All six model parameters were set free for fitting within the following bounds: $a, b, c, d \in [-2, 2]$; $\delta \in$

$[-0.02, 0.02]$; $\beta \in [-0.0002, 0.0002]$. The order of magnitude of the bounds (linear ~ 1 , quadratic ~ 0.01 , cubic ~ 0.0001) was determined by dimensional considerations. We checked afterwards that the obtained distributions were not artifactually truncated by the set bounds.

Hyperparameter values for Differential Evolution were: $mutation = (0.5, 1)$, $recombination = 0.7$, $polish = False$, $workers = -1$, $maxiter = 200$, $popsize = 100$, $tol = 0.03$, $disp = True$.

Our model doesn't include a constant baseline that is usually found in the experimental data [7, 9]. In order to improve fitting, a constant baseline was added to the model variable p_n in each condition. Its value is equal to the average asynchrony in the preperturbation region ($n < 0$) and the average asynchrony in the postperturbation region ($n \geq 7$). For plotting purposes, the preperturbation baseline was shifted to zero by subtracting its average value.

Model fitting was performed as follows, according to our rationale in the Results section:

Perturbation type	Observations and context
SC pure, PS pure	Separate fittings (section II C)
SC comb, PS comb	Separate fittings (section II D)
SC pure, PS pure	Joint fitting (section II E)
SC comb, PS comb	Joint fitting (section II E)

In each case, the two perturbation signs (pos/neg) and the two perturbation sizes (20 ms/50 ms) were included in the fitting.

5. Parameter distributions

Two hundred independent fittings were performed for each case (shown in the previous section), and the distributions of the resulting parameters were analyzed. In particular, the distributions of parameter a were studied for the conditions SC in pure context, PS in pure context, joint fitting for PS and SC in pure context, SC in combined context, PS in combined context, and joint fitting for PS and SC in combined context.

For the SC in pure context, joint fitting for PS and SC in pure context, and joint fitting for PS and SC in combined context cases, distinct subsets of values for the parameter a were observed within the total population, which we call subpopulations (not shown). Two subpopulations were observed for SC in pure context, two for joint fitting for PS and SC in pure context, and two for joint fitting for PS and SC in combined context. The boundaries between these subpopulations were established at SC in pure context: $a = 0.4$, joint fitting for PS and SC in pure context: $a = 0.75$, and joint fitting for PS and SC in combined context: $a = 0.8$.

We removed outliers in parameter a by using the standard Tukey's fences algorithm: a value is detected as outlier if it is outside the interval $[Q_1 - 1.5 \text{ IQR}; Q_3 +$

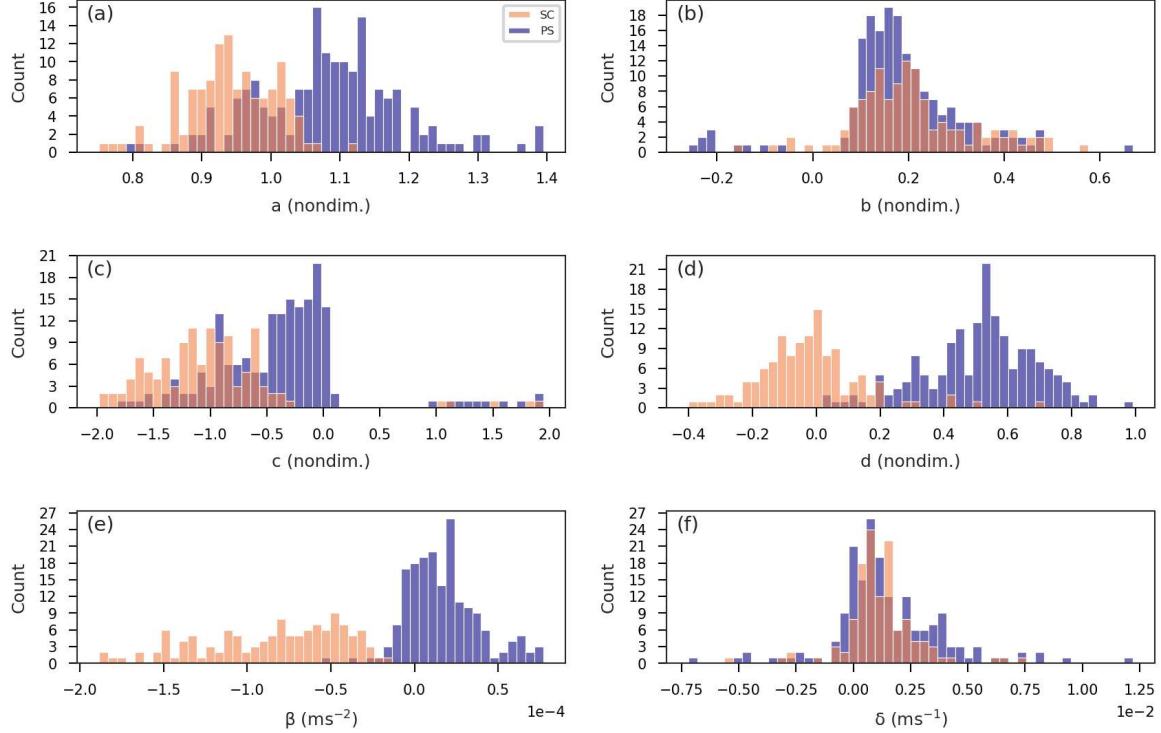


FIG. 6. Separate model fittings to SC in pure context and PS in pure context don't share common parameter values for all parameters (all six model parameters plotted).

1.5 IQR], where $Q_{1,3}$ are the first and third quartiles of the distribution and IQR is the interquartile range. The same criteria were used to detect outliers in the β parameter for PS in pure context and SC in pure context.

6. Solution compatibility

The resulting subpopulations were plotted together (SC in pure context vs PS in pure context and SC in combined context vs PS in combined context). We defined two perturbation types as compatible if their parameter distributions after separate fittings are overlapped to some extent. To quantify the overlapping, the O_{obs} index was defined, which measures the percentage of common values between two populations of the same parameter, belonging to different types of perturbation within the same context.

The O_{obs} calculation considered the common range of values between both distributions, divided into 30 bins. The total number of data points with common bins (*total_common*) was counted and normalized by the total number of data points (*total_data*), obtaining:

$$O_{obs} = (\text{total_common}/\text{total_data}) \times 100 \quad (\text{A5})$$

7. Distribution of distances and statistical analysis

The distributions of the variable *dist* were plotted, especially for the joint fitting for PS and SC in pure context and joint fitting for PS and SC in combined context conditions (see Figure 5). To evaluate the significance of the differences between the two populations, a two-tailed Mann-Whitney-Wilcoxon test was applied.

The following were defined: Pure group (*dist* values from the pure context); Combined group (*dist* values from the combined context); n_1 and n_2 , respective sample sizes.

The Mann-Whitney U statistics and *p*-value were calculated, as well as the effect size δ_{Cliff} , given by:

$$\delta_{Cliff} = \frac{2U}{n_1 n_2} - 1 \quad (\text{A6})$$

A bootstrap was performed with 10,000 iterations to estimate the mean of δ_{Cliff} and its 95% confidence interval (CI).

8. Parameter correlations and incompatibilities

Here we show that parameter interdependence (correlation) is not an issue when concluding about incom-

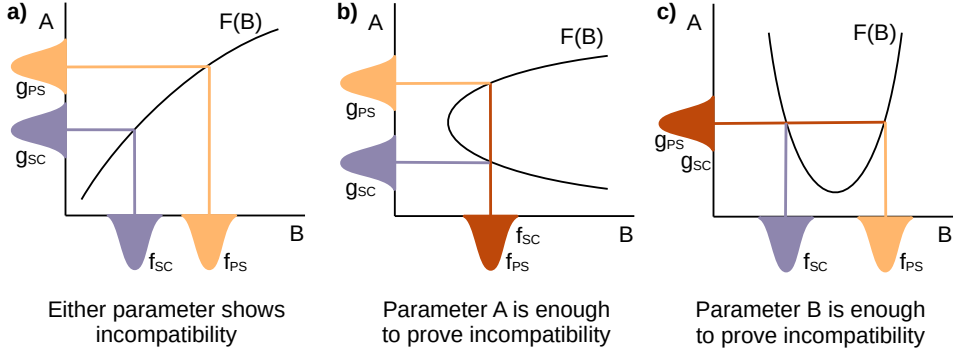


FIG. 7. Correlation between parameters (parameter interdependence) is not an issue when concluding about incompatibility of solutions. (a) Monotone, single-valued correlation. (b) Monotone, multi-valued correlation. (c) Non-monotone, single-valued correlation.

patibility between models based on the non-overlapping obtained distributions.

Consider strictly correlated parameters A and B ; that is, A can be substituted by a function of B : $A = F(B)$. Consider the comparison between SC and PS in pure contexts as in section II C, and assume that the obtained distributions of parameter B are f_{SC} and f_{PS} , respectively. The corresponding distributions of parameter A are g_{SC} and g_{PS} . For the sake of this analysis, consider the following three scenarios depicted in Figure 7:

1. Function F is monotone and single-valued (Figure 7a). If f_{SC} and f_{PS} are non-overlapping, then g_{SC} and g_{PS} are also non-overlapping. Then the incompatibility arises from either parameter. That is, we will find incompatibility either in both parameters or none of them.

2. Function F is monotone and multi-valued (Figure 7b). If f_{SC} and f_{PS} are overlapping, it could still be the case that g_{SC} and g_{PS} are non-overlapping. In this case, parameter A would be enough to prove incompatibility.
3. Function F is non-monotone (Figure 7c). If f_{SC} and f_{PS} are non-overlapping, then g_{SC} and g_{PS} could be overlapping. In this case, parameter B would be enough to prove incompatibility.

Thus, regardless of the particular form of the potential correlation between parameters A and B , any sign of non-overlapping distributions of either parameter would suffice to prove incompatibility.

[1] A. Tsao, S. A. Yousefzadeh, W. H. Meck, M.-B. Moser, and E. I. Moser, The neural bases for timing of durations, *Nature Reviews Neuroscience* **23**, 646 (2022).

[2] H. Hogendoorn, Perception in real-time: predicting the present, reconstructing the past, *Trends in Cognitive Sciences* **26**, 128 (2022).

[3] T. Monteiro, F. S. Rodrigues, M. Pexirra, B. F. Cruz, A. I. Gonçalves, P. E. Rueda-Orozco, and J. J. Paton, Using temperature to analyze the neural basis of a time-based decision, *Nature Neuroscience* **26**, 1407 (2023).

[4] J. J. Paton and D. V. Buonomano, The neural basis of timing: distributed mechanisms for diverse functions, *Neuron* **98**, 687 (2018).

[5] G. Buzzi, F. Eustache, S. Droit-Volet, P. Desaunay, and T. Hinault, Towards a neurodevelopmental cognitive perspective of temporal processing, *Communications Biology* **7**, 987 (2024).

[6] H. K. Inagaki, S. Chen, K. Daie, A. Finkelstein, L. Fontolan, S. Romani, and K. Svoboda, Neural algorithms and circuits for motor planning, *Annual Review of Neuroscience* **45**, 249 (2022).

[7] B. H. Repp, Sensorimotor synchronization: A review of the tapping literature, *Psychonomic Bulletin & Review* **12**, 969 (2005).

[8] B. H. Repp and Y.-H. Su, Sensorimotor synchronization: a review of recent research (2006–2012), *Psychonomic Bulletin & Review* **20**, 403 (2013).

[9] M. L. Bavassi, E. Tagliazucchi, and R. Laje, Small perturbations in a finger-tapping task reveal inherent non-linearities of the underlying error correction mechanism, *Human Movement Science* **32**, 21 (2013).

[10] C. R. González, M. L. Bavassi, and R. Laje, Response to perturbations as a built-in feature in a mathematical model for paced finger tapping, *Physical Review E* **100**, 062412 (2019).

[11] A. D. Silva and R. Laje, Perturbation context in paced finger tapping tunes the error-correction mechanism, *Scientific Reports* **14**, 27473 (2024).

[12] D. R. Roalf, P. Rupert, D. Mechanic-Hamilton, L. Brennan, J. E. Duda, D. Weintraub, J. Q. Trojanowski, D. Wolk, and P. J. Moberg, Quantitative assessment of finger tapping characteristics in mild cognitive impairment, alzheimer's disease, and parkinson's disease, *Journal of Neurology* **265**, 1365 (2018).

[13] A. Von Schnehen, L. Hobeika, D. Huvent-Grelle, and S. Samson, Sensorimotor synchronization in healthy ag-

ing and neurocognitive disorders, *Frontiers in Psychology* **13**, 838511 (2022).

[14] D. Surangsirat, P. Sri-Iesaranusorn, A. Chaiyaroj, P. Va-teekul, and R. Bhidayasiri, Parkinson's disease severity clustering based on tapping activity on mobile device, *Scientific Reports* **12**, 3142 (2022).

[15] S. Williams, D. Wong, J. E. Alty, and S. D. Relton, Parkinsonian hand or clinician's eye? finger tap bradykinesia interrater reliability for 21 movement disorder experts, *Journal of Parkinson's Disease* **13**, 525 (2023).

[16] V. Koppelmans, B. Silvester, and K. Duff, Neural mechanisms of motor dysfunction in mild cognitive impairment and alzheimer's disease: A systematic review, *Journal of Alzheimer's Disease Reports* **6**, 307 (2022).

[17] V. Koppelmans, M. F. Ruitenberg, S. Y. Schaefer, J. B. King, J. M. Hoffman, A. F. Mejia, T. Tasdizen, and K. Duff, Delayed and more variable unimanual and bimanual finger tapping in alzheimer's disease: associations with biomarkers and applications for classification, *Journal of Alzheimer's Disease* **95**, 1233 (2023).

[18] C. R. Ilardi, A. Iavarone, M. La Marra, T. Iachini, and S. Chieffi, Hand movements in mild cognitive impairment: Clinical implications and insights for future research, *Journal of Integrative Neuroscience* **21**, 67 (2022).

[19] K. D. Rudd, K. Lawler, M. L. Callisaya, and J. Alty, Investigating the associations between upper limb motor function and cognitive impairment: a scoping review, *GeroScience* **45**, 3449 (2023).

[20] M. Rosso, B. Moens, M. Leman, and L. Moumdjian, Neural entrainment underpins sensorimotor synchronization to dynamic rhythmic stimuli, *NeuroImage* **277**, 120226 (2023).

[21] L. Bavassi, J. E. Kamienkowski, M. Sigman, and R. Laje, Sensorimotor synchronization: neurophysiological markers of the asynchrony in a finger-tapping task, *Psychological Research* **81**, 143 (2017).

[22] S. L. López and R. Laje, Spatiotemporal perturbations in paced finger tapping suggest a common mechanism for the processing of time errors, *Scientific Reports* **9**, 17814 (2019).

[23] H. Haken, J. S. Kelso, and H. Bunz, A theoretical model of phase transitions in human hand movements, *Biological Cybernetics* **51**, 347 (1985).

[24] J. D. Loehr, E. W. Large, and C. Palmer, Temporal coordination and adaptation to rate change in music performance., *Journal of Experimental Psychology: Human Perception and Performance* **37**, 1292 (2011).

[25] S. W. Egger, N. M. Le, and M. Jazayeri, A neural circuit model for human sensorimotor timing, *Nature Communications* **11**, 3933 (2020).

[26] E. W. Large, I. Roman, J. C. Kim, J. Cannon, J. K. Pazdera, L. J. Trainor, J. Rinzel, and A. Bose, Dynamic models for musical rhythm perception and coordination, *Frontiers in Computational Neuroscience* **17**, 1151895 (2023).

[27] C. Lainscsek, P. Rowat, L. Schettino, D. Lee, D. Song, C. Letellier, and H. Poizner, Finger tapping movements of parkinson's disease patients automatically rated using nonlinear delay differential equations, *Chaos: An Interdisciplinary Journal of Nonlinear Science* **22** (2012).

[28] I. R. Roman, A. Washburn, E. W. Large, C. Chafe, and T. Fujioka, Delayed feedback embedded in perception-action coordination cycles results in anticipation behavior during synchronized rhythmic action: A dynamical systems approach, *PLoS Computational Biology* **15**, e1007371 (2019).

[29] I. Konvalinka, P. Vuust, A. Roepstorff, and C. Frith, A coupled oscillator model of interactive tapping, in *7th Triennial Conference of European Society for the Cognitive Sciences of Music (ESCOM)* (University of Jyväskylä, 2009) pp. 242–245.

[30] O. A. Heggli, J. Cabral, I. Konvalinka, P. Vuust, and M. L. Kringelbach, A kuramoto model of self-other integration across interpersonal synchronization strategies, *PLoS Computational Biology* **15**, e1007422 (2019).

[31] P. Słowiński, K. Tsaneva-Atanasova, and B. Krauskopf, Effects of time-delay in a model of intra-and interpersonal motor coordination, *The European Physical Journal Special Topics* **225**, 2591 (2016).

[32] R. Gilmore, Topological analysis of chaotic dynamical systems, *Reviews of Modern Physics* **70**, 1455 (1998).

[33] Y. Chen, M. Ding, and J. S. Kelso, Long memory processes ($1/f^\alpha$ type) in human coordination, *Physical Review Letters* **79**, 4501 (1997).

[34] See Supplemental Material at [URL-will-be-inserted-by-publisher] for supplementary figures.

[35] R. M. Reitan and D. Wolfson, Theoretical, methodological, and validation bases of the Halstead-Reitan neuropsychological test battery, in *Comprehensive Handbook of Psychological Assessment* (John Wiley & Sons, Ltd, 2003) Chap. 8, pp. 105–131.

[36] B. H. Repp, Automaticity and voluntary control of phase correction following event onset shifts in sensorimotor synchronization., *Journal of Experimental Psychology: Human Perception and Performance* **28**, 410 (2002).

[37] B. H. Repp and P. E. Keller, Adaptation to tempo changes in sensorimotor synchronization: Effects of intention, attention, and awareness, *The Quarterly Journal of Experimental Psychology Section A* **57**, 499 (2004).

[38] J. A. Michaels, M. Kashefi, J. Zheng, O. Codol, J. Weiler, R. Kersten, J. C. Lau, P. L. Gribble, J. Diedrichsen, and J. A. Pruszhynski, Sensory expectations shape neural population dynamics in motor circuits, *Nature* , 1 (2025).